

Development and deployment of a Delphes based simulation in the LHCb simulation framework Gauss

A. Davis¹, B. Siddi².

¹*University of Manchester, Manchester, UK*

²*INFN Sezione di Ferrara, Ferrara, Italy*

Abstract

Faster alternatives to a full, GEANT4-based simulation are being pursued within the LHCb experiment. In this context, the integration of the Delphes toolkit in the LHCb simulation framework is intended to provide a fully parameterized option. This document presents the current status of the Delphes toolkit in Gauss, the LHCb simulation framework. In this integration, the particle transport performed by GEANT4 and subsequent mimicking of detector response and reconstruction has been replaced with a parametric response of the various detector elements. The implementation required significant changes to Delphes itself to constrain the particle transport inside the detector acceptance and to match the LHCb dipole magnetic field. The configuration of various parameterizations of resolution and efficiency is also tuned to provide a fully functional LHCb simulation. The output of the resulting fast simulation is formatted to be used directly in the LHCb physics analysis framework DaVinci.

1 Introduction

In LHCb, the interactions of particles with the detector elements are simulated in detail with the GEANT4 toolkit. This kind of simulation requires huge computing resources; therefore the generation of large Monte Carlo samples is usually slow and CPU-intensive. However, there are cases such as feasibility studies, detector design, and evaluation of systematic uncertainties in the final phases of analyses, where a high level of complexity is not required; a simplified approach based on the parameterization of the detector response is sufficient. The DELPHES framework [1] is designed to implement a parameterized simulation in an arbitrary High Energy Physics experiment. Starting from common event generator outputs, it performs a fast and realistic simulation of a general purpose collider detector. The particle energies are computed by smearing the initial visible particles momenta according to the detector resolution in a highly-customizable way. As a result most particles and detector effects can be reconstructed and reproduced. DELPHES was originally developed for general-purpose detectors as CMS and ATLAS.

A generalized parametric Monte Carlo tool was not available up to now in the LHCb experiment and the DELPHES toolkit has been chosen to provide this kind of functionality. The main steps to make DELPHES available in the LHCb software environment is to integrate it in the LHCb simulation framework, GAUSS [2], and bypassing the particle transport performed by GEANT4, in order to provide all the physical quantities and LHCb variables necessary for physics analysis. Moreover, a careful implementation of the DELPHES plugin allows parameterization of only parts of the simulation sequence, while keeping fully-detailed simulation for the rest. For example, an efficient and realistic hybrid simulation could be made by fully simulating charged particle tracking, and by a fast parameterization of calorimetry and particle identification. A correct LHCb detector parameterization is fundamental to obtain a correct physical output using DELPHES; this is achieved by looking at the full detector simulation as well as real data control samples, and extrapolating the parameters to be used. The DELPHES implementation in LHCb provides a faster way to generate high-statistics samples, but would also be extremely helpful in designing possible future detectors. Such studies are already underway for use in the LHCb Upgrade-II calorimeter, specifically in design aspects concerning detector granularity, timing resolution and layout.

This document presents the interface of DELPHES within the GAUSS and the subsequent processing sequence, following in the order of the DELPHES sequence itself. We present in the following sections the general implementation, followed by the description of the particle transport inside the LHCb acceptance, then the parameterization of resolution and efficiency for charged particle tracking; the efficiency and misidentification of particle identification, and the calorimeter. The fast simulation output has been formatted in order to be directly used in the LHCb physics analysis framework DAVINCI. We also present in this document the timing of the sequence and a few examples of the physics performance.

2 Delphes in LHCb

2.1 Implementation of Delphes Within Gauss

As Delphes is a stand alone package, the calling of it within Gauss must be done similarly to other packages. Therefore we try to adopt the same strategy of integration as Geant4 [3]. To this end, the Delphes github repository, found at <https://github.com/delphes/delphes> is mirrored within the LHCb Gitlab framework at <https://gitlab.cern.ch/lhcb/delphes-srcs>. This mirroring allows for individual patches necessary for the LHCb implementation to be applied on top of any outwardly maintained Delphes branch. For the purposes of development, we have been using the Delphes 3.4.1 branch, as it is still the latest release. At `cmake` configuration time, the path to a local installation of Delphes is searched for; if any local configuration is not found, then at build and compile time, the Delphes project is cloned from the `delphes-srcs` repository and the specific changes, discussed in Section 3.¹

2.2 Output for physics analysis

In the context of the LHCb simulation framework, DELPHES will substitute the detailed simulation performed by GEANT4, and will give as output only high level reconstructed objects. In Figure 1 a schematic view of the chain from generation to analysis in LHCb is given. Offline analyses in LHCb are performed using the DAVINCI software package [?]. The DAVINCI application allows for reconstructed particles to be combined and kinematic quantities, such as invariant masses of decayed particles and their distance of flight. It takes as input reconstructed basic objects and it is possible to create new particles which are composed of said basic object and to perform candidate selection. Since the hits in the detector are not simulated, the reconstruction cannot be run; therefore the output from DELPHES must provide directly objects expected by the analysis tool DAVINCI. The minimal output that can be given to the analysis software is the `LHCb::ProtoParticle`². This is a high level reconstructed object containing information for particles, such as:

- Links with tracks;
- At least one particle ID information;
- Link to calorimeter objects;
- Link to particle ID hypothesis objects.
- The relevant covariance matrices
- The track χ^2/ndf
- The ghost probability
- PID response objects

¹The possibility of having a local installation of Delphes is accomplished by setting the `CMAKE_PREFIX_PATH` to point to the local installation of Delphes. NB: Compiling with the same environment as the rest of Gauss is strongly recommended to avoid compatibility/linking issues.

²We note that this is for the Run I and II event model. Should the event model change in the future, this structure will then need to change.

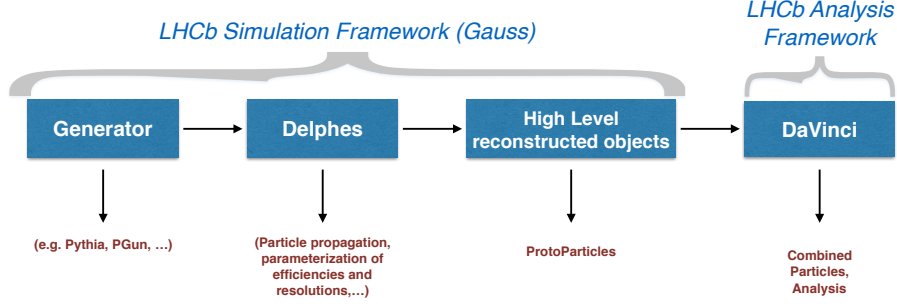


Figure 1: Schematic view of the chain from generation to analysis in LHCb.

75 The standard DELPHES workflow concerning the module configuration is schematized
 76 in Fig.2.

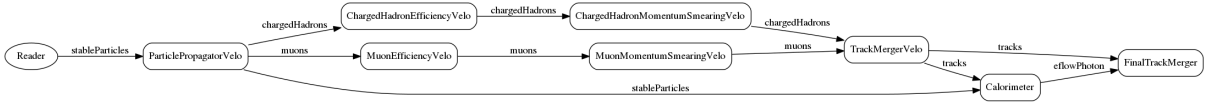


Figure 2: Schematic view of the modules configuration.

77 In the following sections a detailed description of the customized modules for LHCb
 78 will be presented.

79 3 Custom LHCb modules

80 In this section, a detailed description of the customized modules for LHCb are presented.

81 3.1 LHCb Particle Propagator

82 The default DELPHES particle propagator module has been written for a solenoidal
 83 magnetic field embedded in a cylindrical acceptance. It was therefore necessary to write
 84 new code to add functionality to match the LHCb acceptance. The propagation is made
 85 with a simple transport into a dipole field assuming a mean value for the shift of the
 86 transverse momentum component of the particles, known as the $p_x - kick$ or single bend
 87 point approximation; this is similar to what is done in the pattern recognition for transport
 88 between the VELO and T stations for long tracks, or vice-versa. Nevertheless, the point
 89 in which the $p_x - kick$ is applied has been parameterized as function of the inverse of the
 90 momentum of each particle, $Z_{MagnetCenter} \propto \left(\frac{1}{p}\right)^2$, as shown in Fig.3; The main principle
 91 of the particle propagator is to perform an acceptance check at various z of the LHCb
 92 detector. It proceeds in the following way:

- 93 1. Check if the final state particle produced is in the LHCb Detector "box" of allowed
 94 angles, e.g., $12 < |t_x| < 300$ and $12 < |t_y| < 250$;
- 95 2. an effective z coordinate of the magnet center "felt" by the charged particle is
 96 parameterized with a second order equation as function of $1/p$. This value can be
 97 given by a second order function or a fixed coordinate taken as external input;

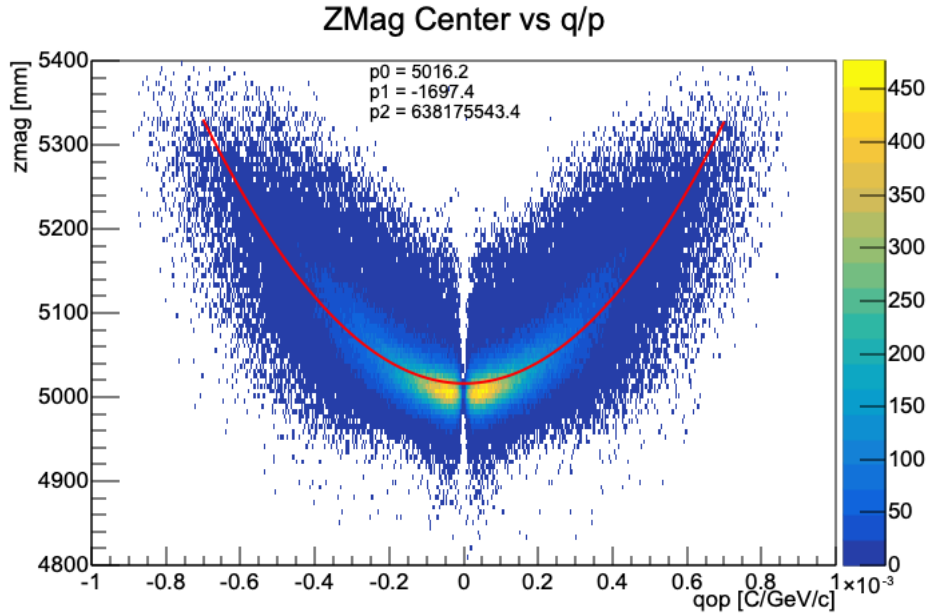


Figure 3: Magnet center parameterization.

- 98 3. particles are propagated until the corresponding magnet center;
- 99 4. A momentum kick in the transverse direction, i.e. p_x , is given to charged particle.
- 100 The mean value has been computed comparing the p_x component of the momentum
- 101 at two z , one before the magnet, i.e. at the end of the VELO, and one after, i.e. at
- 102 the calorimeter entrance. The result is shown in Fig.4;
- 103 5. after the kick, another check is done to see if the particle is still in the acceptance of
- 104 the LHCb detector at the end of the T stations.

105 The acceptance is then divided into three regions:

- 106 • In acceptance before the magnet and not after;
- 107 • In acceptance after the magnet and not before;
- 108 • In acceptance along the whole detector.

109 Particles are then saved in corresponding containers such as:

```

110 fOutputArray =
111     ExportArray(GetString("OutputArray", "stableParticles"));
112 fOutputArrayUpstream =
113     ExportArray(GetString("OutputArrayUpstream", "upstreamParticles"));
114 fOutputArrayDownstream =
115     ExportArray(GetString("OutputArrayDownstream", "downstreamParticles"));
116
117 fChargedHadronOutputArray =
118     ExportArray(GetString("ChargedHadronOutputArray", "chargedHadrons"));
119 fChargedHadronOutputUpstreamArray =
120     ExportArray(GetString("ChargedHadronOutputUpstreamArray", "upstreamchargedHadrons"));
121 fChargedHadronOutputDownstreamArray =
122     ExportArray(GetString("ChargedHadronOutputDownstreamArray", "downstreamchargedHadrons"));
123
124 fElectronOutputArray =
125     ExportArray(GetString("ElectronOutputArray", "electrons"));
126 fElectronOutputUpstreamArray =
127     ExportArray(GetString("ElectronOutputUpstreamArray", "upstreamelectrons"));
128 fElectronOutputDownstreamArray =
129     ExportArray(GetString("ElectronOutputDownstreamArray", "downstreamelectrons"));
130

```

```

131 fMuonOutputArray =
132     ExportArray(GetString("MuonOutputArray", "muons"));
133 fMuonOutputUpstreamArray =
134     ExportArray(GetString("MuonOutputUpstreamArray", "upstreammuons"));
135 fMuonOutputDownstreamArray =
136     ExportArray(GetString("MuonOutputDownstreamArray", "downstreammuons"));
137
138 fNeutralOutputArray =
139     ExportArray(GetString("NeutralOutputArray", "neutrals"));
140 fNeutralOutputUpstreamArray =
141     ExportArray(GetString("NeutralOutputUpstreamArray", "upstreamneutrals"));
142 fNeutralOutputDownstreamArray =
143     ExportArray(GetString("NeutralOutputDownstreamArray", "downstreamneutrals"));
144
145 fPhotonOutputArray =
146     ExportArray(GetString("PhotonOutputArray", "photons"));
147 fPhotonOutputUpstreamArray =
148     ExportArray(GetString("PhotonOutputUpstreamArray", "upstreamphotons"));
149 fPhotonOutputDownstreamArray =
150     ExportArray(GetString("PhotonOutputDownstreamArray", "downstreamphotons"));

```

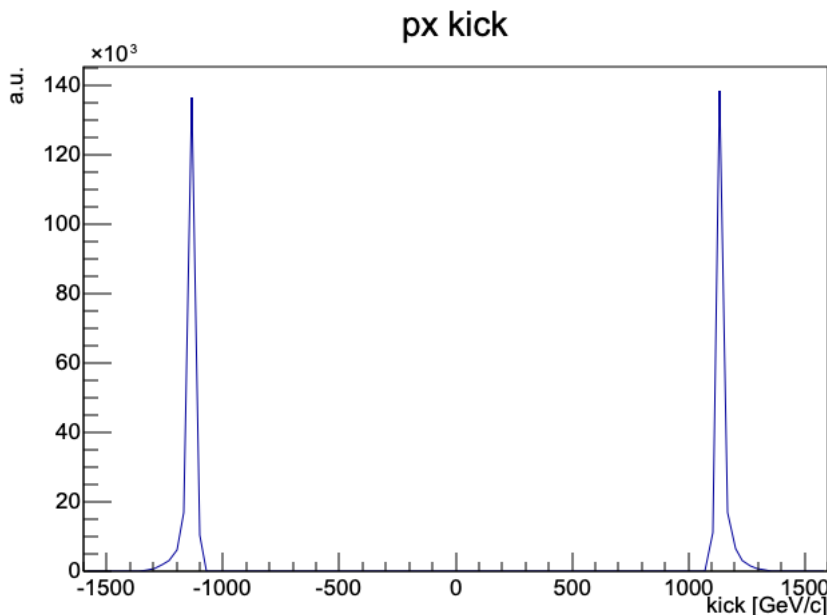


Figure 4: p_x kick distribution for charged positive and negative particles.

151 Correlations with the track slopes were searched for using full Monte Carlo simulation,
152 but were found to be negligible. Should this no longer be the case, as may very well be with
153 either mis-alignments, change of detector, or otherwise, the change in parameterization is
154 easily set as a formula in the DELPHES configuration card.

155 3.2 Efficiency

156 Tracking resolutions and efficiencies are obtained from the LHCb detailed simulation.
157 To include these in DELPHES, two dedicated DELPHES modules have been developed
158 which take as input histograms providing the parameterization for the LHCb detector.
159 Efficiencies are taken as reconstructed tracks in the tracker acceptance. The resolution is
160 defined as the root mean square of differences between reconstructed Monte Carlo tracks
161 and the Monte Carlo truth. The kinematic variables adopted to fill both histograms are
162 the track slopes $t_x = p_x/p_z$, $t_y = p_y/p_z$ and the inverse of the particle momentum $1/p$.
163 Figure 5 shows the comparison between DELPHES and detailed simulation output for
164 the t_x , t_y and $1/p$ variables used for the parameterization. A specific parameterizations

165 for each data taking period and detector conditions will be provided as full simulation
 166 becomes available. The procedure is described in Sec.3.4.

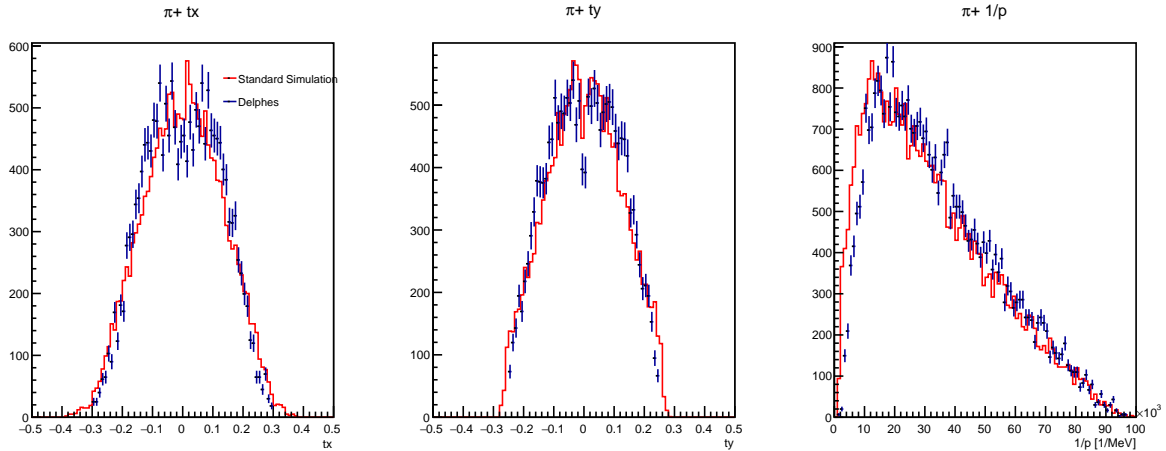


Figure 5: Track slopes $t_x = p_x/p_z$, $t_y = p_y/p_z$ and $1/p$ comparison between standard simulation and DELPHES.

167 The original efficiency module has been rewritten in order to take as input two 3D
 168 histograms. The efficiency is obtained in the following way:

- 169 1. Input of two TH3D histograms (Reconstructed/Reconstructible) binned in t_x , t_y
 170 and $1/p$ (same z and acceptance cuts as in particle propagator);
- 171 2. X , Y , Z projections of Numerator/Denominator histograms;
- 172 3. Compute histogram ratio of each projection (hx_eff , hy_eff , hz_eff)

173 Then at the execution time the efficiency is applied doing:

- 174 1. Take candidate Lorentz momentum vector;
- 175 2. Compute t_x , t_y and $1/p$;
- 176 3. Search t_x , t_y and $1/p$ associated bin in hx_eff , hy_eff , hz_eff ;
- 177 4. Take the efficiency in each bin;
- 178 5. Generate a uniform random number $[0,1]$;
- 179 6. If random number $>$ the *or* of each efficiency \rightarrow skip the event.

180 3.3 Resolution Smearing

181 As for the new efficiency module, the resolution smearing module has been written to
 182 take as input a 6D histogram binned as follow: Monte Carlo truth distributions of t_x ,
 183 t_y , and p , differences between the reconstructed and the Monte Carlo truth of the same
 184 variables in the last 3 axis. At execution time the smearing is applied in this way:

- 185 1. Take candidate four-momentum vector as a TLorentzVector;

- 186 2. Compute t_x and t_y ;
- 187 3. Find corresponding t_x , t_y and p bin in `THnSparse` histo;
- 188 4. Set `THnSparse` corresponding range in t_x , t_y and p ;
- 189 5. Retrieve (True-Rec) `THnSparse` projections;
- 190 6. Compute RMS for each projection;
- 191 7. Generate Gaussian distributed random number with $\mu = var$, $\sigma = RMS$;
- 192 8. Assign new value to t_x , t_y and p .

193 3.4 Efficiencies and resolutions histograms

194 A custom python script is used to construct the efficiency and resolution histograms, re-
 195 spectively two `TH3D` for efficiency (reconstructed and reconstructible) and a 6D `THnSparse`
 196 for resolution, and to save them into a `ROOT` file. It takes as input a `TTree`, described in
 197 Sec.3.5, containing several track quantities computed at a given z coordinate necessary to
 198 fill the histograms. The workflow is the following:

- 199 1. reduce the trees with the cuts: same acceptance cut on t_x , t_y at the origin of the
 200 particle;
- 201 2. loop over the trees;
- 202 3. fill `THnSparse` and `TH3D`:
 - 203 • 6D `THnSparse` binned in true t_x , t_y , p and true-rec t_x , t_y , p ;
 - 204 • two `TH3D` binned in t_x , t_y , p both reconstructed and reconstructible
- 205 4. write to file.

206 3.5 Custom Brunel algorithm

207 The `TTree` is created by the algorithm `TrackEffRes.{cpp,h}` embedded in `Tr/-`
 208 `TrackChecker` tools of the `Rec` package. (see branch `WIP_addTrackEffRes_forDelphes` in
 209 `LHCb/Rec` repository). The algorithm proceeds as follows:

- 210 1. loops over the `LHCb::MCParticles` container;
- 211 2. for each `LHCb::MCParticle` several quantities (e.g. p_x , p_y , $mass$) are saved at
 212 different z coordinate (this is done thanks to a track extrapolator tool) into a `TTree`
- 213 3. a check if the `LHCb::MCParticle` correspond to a reconstructible and reconstructed
 214 track the same quantities are saved into other two `TTrees`
- 215 4. the trees are saved into a `ROOT` file used as input to other algorithms

216 3.6 Implementation of the LHCb calorimeter in Delphes

217 As with the magnetic field, DELPHES itself was designed to treat the calorimeter in bins
218 of η and ϕ , exploiting the cylindrical symmetry of a general purpose detector. As this is
219 clearly not suited to the LHCb geometry, as in the case of the particle propagation module,
220 we opt instead to use this as a base to build our own calorimeter module which instead uses
221 Cartesian coordinates. This was first implemented by Zehua Xu in the `CalorimeterLHCb`
222 module, which has been simplified and included in the `delphes-src` repository. The great
223 strengths of this module are two-fold: First, as the LHCb calorimeter is made of repeating
224 cuboid towers, we can use one simple *tower* as a building block, and execute three simple
225 loops within the definition of the card itself to create the entire LHCb calorimeter. Second,
226 the module is completely replaceable without hurting the overall framework of DELPHES
227 or GAUSS, meaning that if a better model of shower formation is possible, it is easily
228 implemented.

229 For each photon that is propagated to the calorimeter face, the energy is smeared by
230 the resolution of the LHCb calorimeter measured in test-beam data, $\frac{\sigma(E)}{E} = \alpha/\sqrt{E} \oplus \beta$,
231 with $\alpha = 10\%$, $\beta = 1\%$ [4]. The energy smearing was only limited to one tower per hit, then
232 the subsequent smearings between cells are done after the return of the tower itself from
233 DELPHES to GAUSS in the `DelphesCaloProto` algorithm. In the current implementation,
234 only photons are considered, with the possibility of extension to neutral hadrons foreseen
235 with adequate tuning.

236 3.7 Python Configuration

237 In the following sections, we describe how we fulfill the criteria stated in Section 2.2. It
238 is easiest to understand by walking through the logic of the DELPHES sequence within
239 GAUSS, which is defined by the configuration of the python options. This is given by (and
240 listed in `Sim/LbDelphes/options/LbDelphes.py`):

- 241 • `DelphesAlg`: Algorithm which takes as input HEPMC particles, passes the col-
242 lection to DELPHES, which then performs the particle propagation, smearing and
243 efficiency, then returns the result; this result is then packaged and output as
244 `LHCb::MCParticles`
- 245 • `DelphesHist`: Histogramming for monitoring after `DelphesAlg`. This tool is histor-
246 ical, and has been deprecated in favor of `DelphesTuple`.
- 247 • `DelphesProto` converts the charged `LHCb::MCParticles` into
248 `LHCb::ProtoParticles`
- 249 • `DelphesRecoSummary`, which adds to the TES the `LHCb::RecSummary` information
250 needed for calculation of RICH and Muon response. In its simplest version, it
251 draws a random number of tracks from a histogram defined via the `Configurables`
252 and stores it into a newly created `LHCb::RecSummary` object; in the future it will
253 be extended to randomize the number of reconstructed tracks (`nTracks`) as a function
254 of the number of charged particles at generator level;
- 255 • `DelphesParticleId`, which computes the detector response of the RICH and Muon
256 detectors and loads it in the `LHCb::RichPID` and `LHCb::MuonPID` objects; the

257 Configurable of `DelphesParticleId` allows to define the paths in the filesystem to
258 the TensorFlow models modelling the Rich detector differential log likelihoods, the
259 efficiency of the `isMuon` criterion and the differential log-likelihoods obtained from
260 the Muon system; the description of the neural network models and the interface
261 between Gaudi and discussed in a dedicated note [5];

- 262 • `ChargedProtoParticleAddRichInfo`, which loads the RICH log-likelihoods from
263 the `LHCb::RichPID` objects to the `LHCb::ProtoParticle` as an `additionalInfo`
264 flag
- 265 • `ChargedProtoParticleAddMuonInfo`, which loads the `isMuon` and Muon log-
266 likelihoods from the `LHCb::MuonPID` objects to the `LHCb::ProtoParticle` as an
267 `additionalInfo`
- 268 • `ChargedProtoCombineDLLsAlg`, which combines the Rich, the Calorimeter (if
269 available) and the Muon log-likelihoods into the Combined DLLs, commonly
270 used at analysis level to define particle identification criteria; as the algorithms
271 `ChargedProtoParticleAddRichInfo` and `ChargedProtoParticleAddMuonInfo`,
272 `ChargedProtoCombineDLLsAlg` is not specific to DELPHES, but is developed and
273 maintained for the reconstruction and selection frameworks (`BRUNEL` and `DAVINCI`),
274 and listed here to reproduce the behaviour of the reconstruction step which para-
275 metric simulation allows to skip
- 276 • `DelphesCaloProto`: This algorithm is responsible for converting the neutral MC
277 particle into usable calorimeter deposits, followed by the production of neutral
278 protoparticles for use in `DAVINCI`
- 279 • `DelphesTuple`: Algorithm which creates an `NTuple` of the results for use in either
280 tuning or `MCParticle` level studies
- 281 • `BooleInit`: provide the ODIN information for DELPHES. This will be deprecated
282 as the algorithm will be moved to the LHCb package and will be accessible across
283 projects.
- 284 • `PgPrimaryVertex`: Provide a PV as with ParticleGun simulations. This package
285 was moved from the `BRUNEL` package to the LHCb package for use across projects.

286 This sequence takes all HEPMC particles and transforms them to the particles used in
287 final analysis level simulation.

288 In the following sections, we describe first the implementation of the DELPHES config-
289 uration, then describe each step that the generated particles see. This follows the logic of
290 the DELPHES sequence, and provides the most natural description of why each algorithm
291 is where it is.

292 3.7.1 Automatic Generation of Delphes Configuration Card File

293 DELPHES is configured via a tcl file called a *card*. This card file defines first the se-
294 quence of execution, then the individual configurations of each of the steps. This
295 includes the particle propagation, resolution and efficiency smearing, as well as the
296 definition of the calorimeter geometry to be used. Instead of forcing all LHCb users

297 to learn tcl, we factor the card definition into a python configurable option, housed
 298 in `Sim/LbDelphes/python/LbDelphes/LbDelphesCardTemplates` called `DelphesCard`.
 299 This file allows one to first configure directly a simple card file for use in all manners
 300 of simulation, and (2) allow for custom modification for expert studies. The default
 301 configuration looks like:

```
302 from LbDelphes.LbDelphesCardTemplates import DelphesCard
303 c = DelphesCard.DelphesCard(name = 'delphes_card',
304                             year = '2012',
305                             magPolarity='up',
306                             efficiencies=True,
307                             resolutions=True
308                             )
309 #configure the card here for expert users
310 #c.modules['ECAL'].custom_xy_binning(...)
311 c.FinalizeCard()
```

312 This is accomplished using python template replacement on the template files included
 313 in the same directory. Three templates are used, namely `module_base.tcl`, which is the
 314 general base input for any DELPHES module, `module_merger.tcl`, which is special, as it
 315 takes multiple inputs and concatenates them into one output, and `module_lhcb_ecal.tcl`,
 316 which is necessary to form the ECAL response. We keep track of the order that the
 317 modules are added within the sequence, to ensure that the python configuration creates
 318 a self-consistent configuration card. We have also left the possibility of extending the
 319 card maker to include options for the future, for instance tracker-only requests would
 320 immediately eliminate the need for the calorimeter configuration.

321 This framework is then completely customizable for expert users, as a new DELPHES
 322 algorithm can be added to the externally compiled DELPHES build, then configured by
 323 the same python options given by the card creator.

324 4 DelphesAlg

325 With the specific DELPHES modules declared, we now discuss the remaining parts of
 326 the sequence. The first is `DelphesAlg`, which is the only algorithm which ever interacts
 327 with DELPHES. The algorithm starts by taking HEPMC events which are written to the
 328 transient event store (TES) and filling them into the input arrays necessary for DELPHES.
 329 At this point, the MC primary vertex is found one of three ways³:

- 330 1. One searches for the beam particles associated to the event, and takes their decay
 331 vertices, if they exist.
- 332 2. The signal process vertex stored in HepMC is used directly
- 333 3. Take the production/end vertex of the particle with barcode 1. This particle is
 334 special.

335 If no PV is found, an error is thrown.

³With thanks to Gloria Corti

336 Once all arrays are filled, the DELPHES object is asked to process the task configured
337 by the tcl card. This uses all the information presented in Sections 2.1-3.6. Once this
338 is completed, we import all results from the final output location of DELPHES back into
339 GAUSS. From here, all LHCb::MCParticles and LHCb::MCVertices are written to the
340 TES.

341 One specific note for DelphesAlg, the variable M2 in the DELPHES Candidate class
342 is constant both before and after the interaction with the DelphesFactory, hence the
343 particle propagation. This provides a good variable to attach the key of a particle to,
344 which is necessary to follow the particle before and after propagation. This is also used as
345 the key in the keyed container of an object.

346 5 DelphesProto

347 DelphesProto is the algorithm dedicated to build the minimal output for charged
348 particles, to be given as input to DAVINCI analysis framework. This consists in
349 LHCb::ProtoParticles, LHCb::Tracks with at least one LHCb::State and basic PID
350 information that will be filled after with dedicated algorithms.

351 DelphesProto algorithm take as input LHCb::MCParticles and LHCb::MCVertices
352 created in the previous step and fill the corresponding quantities into the higher level
353 objects. Covariance error matrix associated to the track is also parameterized. This
354 has been done with a lookup table in which each matrix element has been averaged as
355 function of $1/p$. A very similar procedure is used to fill other track properties such as
356 ghost probability, fit likelihood, track χ^2 and number of degrees of freedom. The track
357 fit information and the covariance matrix are filled with lookup table generated by a
358 standalone script described in Sec.5.1. This last step is done retrieving from the table the
359 row corresponding to a particular $1/p$ range of the particle, then for each entry of the
360 matrix the mean value and the error is used to smear the value to be given to the track.
361 All objects related to tracking are filled and stored in the corresponding TES containers
362 the standard LHCb analysis tools can be used as they are proving the feasibility of the
363 generation to analysis chain. Figure 6 show the invariant mass of two reconstructed pions
364 through DELPHES, obtained with standard LHCb analysis framework. Once all objects
365 related to tracking are filled (covariance matrices, χ^2/ndf), the standard LHCb analysis
366 tools can be used: this proves the feasibility of the generation to analysis chain. Figure 6
367 show the invariant mass of two reconstructed pions through DELPHES, obtained with
368 standard LHCb analysis framework. To perform a direct comparison with the standard
369 simulation the correct parameterization has to be performed and validated. Figure 7
370 presents a comparison of the reconstructed invariant mass of the decay $D_s^+ \rightarrow \phi\pi^+$ with
371 $\phi \rightarrow K^+K^-$ as obtained from the 2016 calibration samples and from DELPHES. The
372 plot was obtained using Bender and DAVINCI to process the simulated and real data
373 samples, respectively. While the simulation slightly underestimates the error on this mass
374 resolution, the level of agreement is already impressive.

375 5.1 Covariance and track information lookup tables

376 Two custom python scripts has been written to create a .dat file containing the mean
377 value and the error of each element that goes inside the lookup table as function of $1/p$.

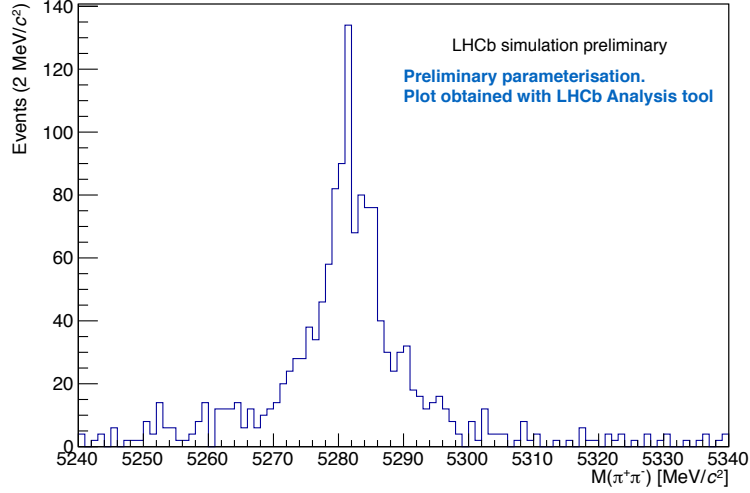


Figure 6: Invariant mass of $\pi^+\pi^-$ combination of the decay $B^0 \rightarrow \pi^+\pi^-$, obtained using final reconstructed objects from the DELPHES sequence in GAUSS to LHCb analysis framework DAVINCI.

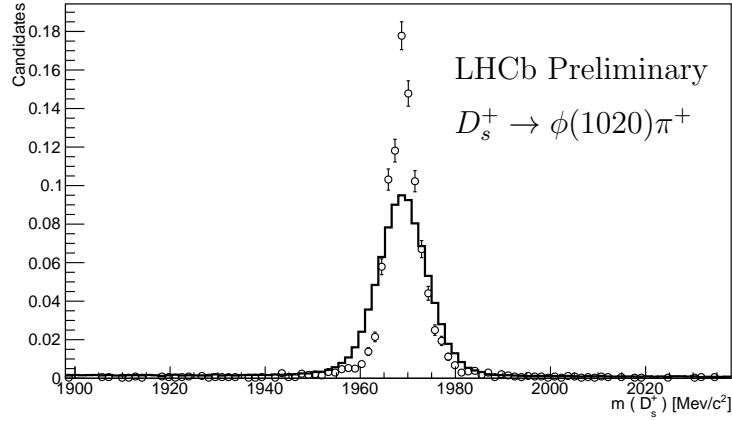


Figure 7: Comparison between the mass resolution of the decay $D_s^+ \rightarrow \phi(\rightarrow K^+K^-)\pi^+$ as obtained from the 2016 calibration samples (solid line) and with the DELPHES smearing (markers with error bars). To reduce the kinematic differences between the two samples, only D_s^+ candidates with p_T between 3 and 4 GeV/c and η between 2.5 and 3.0 have been used in the fit.

378 They take as input a ROOT file with a TTree containing several track quantities computed
 379 at a given z coordinate necessary to fill the table.

380 The structure of the covariance lookup table is the following:

$$381 \quad \min 1/p \mid \max 1/p \mid cov_{0,0} \mid \sigma(cov_{0,0}) \mid cov_{0,1} \mid \sigma(cov_{0,1}) \mid \dots \mid cov_{n,n} \mid \sigma(cov_{n,n})$$

382 The track parameter lookup table structure instead is:

$$383 \quad \min 1/p \mid \max 1/p \mid \chi^2 \mid \sigma(\chi^2) \mid nDOF \mid \sigma(nDOF) \mid \mathcal{L} \mid \sigma(\mathcal{L}) \mid$$

384 In order to compute the entries, the script proceeds in this way:

- 385 1. Create and fill a `TProfile` for each element;
- 386 2. For each bin get the mean and the error;
- 387 3. Save each entry into a `.dat` file

388 The scripts are extendable to have the possibility to include other track parameters.

389 6 DelphesCaloProto

390 The output of DELPHES requires more work to make the proper calorimeter object. There
391 are three major steps in the calorimeter protoparticle maker:

- 392 1. Generate all the showers for the photon individually, ignoring overlap in cells
- 393 2. For each generated shower, sum the energy of overlapping cells to form the total
394 calorimeter response
- 395 3. Now that all contributing cells have the correct energy, compute the covariance
396 matrix and the barycenter of the cell, as calculated in the LHCb framework

397 This defines a maximum of 3 loops over all particles. Should the clustering and overlap
398 be changed to be performed in DELPHES itself, the number of loops over particles would
399 be reduced to one, but with a lack of clarity of overlap in cells.

400 6.1 Smearing of energy to neighboring cells

401 The smearing of energy to neighboring cells is accomplished by Monte Carlo integration.
402 We assume a simple model that the Molière radius R_M well describes the calorimeter
403 shower response. Under this assumption, concentric circles of $1, 2, 3.5R_M$ enclose 90, 95
404 and 99% of the energy of the shower. Therefore, we draw the circles of these Molière radii
405 around the x, y position of the particle at the calorimeter face. This smearing is applied
406 irrespective of whether or not the shower is confined to one region of the calorimeter.
407 At this point, the DELPHES calorimeter module has already smeared the position of the
408 photon hit with respect to the true MC hit. This can be disabled, but has shown good
409 agreement with full simulation for Upgrade II ECAL studies. It is also important to
410 note here that the showering does not take into account the angle of the photon with the
411 calorimeter face. To do this, one should take into account the depth of the calorimeter,
412 then draw two ellipses with the center of each ellipse being the particle trajectory and the
413 other parameters defined by the intersection of the cylinders of said Molière radii with
414 the planes of the calorimeter. This naive approximation completely ignores all structure
415 of the calorimeter itself, but can be tuned.

416 We then include all cells where the energy has been smeared, a cluster, into the next
417 step.

418 6.2 Overlap of clusters

419 For this part, we rely on the fact that energy is a scalar quantity, and can therefore be
420 summed. We then simply take all clusters from the previous step to check for overlapping
421 towers. If the towers overlap, both clusters reset the energy of that tower to be the sum
422 of the energies of each individual tower. This process is done until all clusters have been
423 processed.

424 6.3 Formation of covariance matrices and protoparticles

425 Once all clusters have been formed, one can form all the necessary ingredients for the
426 neutral protoparticles. This relies on a bit of a complicated interaction with the TES at
427 this point, but when moving to `Gaudi::Functional`, it should become much simpler. The
428 first step is to assign all the `LHCb::CaloCellIDs` to their corresponding `LHCb::CaloDigit`
429 with the correct energy associated. These are then put into the TES and accessed from
430 there.

431 Once the digits are formed, the barycenter and covariance matrix of each cluster is
432 calculated. The barycenter is calculated in the usual way, as the energy weighted mean of
433 the cluster, and the covariance is calculated as

$$\sigma_{ij} = \frac{1}{N} \sum_{clusters}^N (\vec{x}_i - \bar{\vec{x}}_i)(\vec{x}_j - \bar{\vec{x}}_j) \quad (1)$$

434 where $\vec{x} = [x, y, E]^T$, the relevant variables for the calorimeter covariance matrix. We
435 leave open the possibility of tuning these variables for possible detector response, but
436 explicitly do not include any response due to the electronics, as in the development of
437 this module, the study of the PhaseII upgrade ECAL was envisioned and the electronics
438 to be used was unknown.

439 With the relevant covariance matrices and barycenters in place, as well as the contrib-
440 uting clusters and seed, we form the relevant `LHCb::CaloPosition`, `LHCb::CaloCluster`
441 and `LHCb::CaloHypo` which finalize the `LHCb::ProtoParticle` for the neutral particle in
442 the calorimeter.

443 7 Timing measurements

444 To estimate the performance increase gain by adopting DELPHES, we run event simulations
445 with the standard GAUSS implementation for 2012, the implementation only using the
446 generation phase, and GAUSS with DELPHES for 200 events. As the performance for
447 timing can vary wildly with the type of decay produced, we choose a collection of decays
448 files, listed in Table 1. This sample is chosen to try to cover many standard use cases.
449 This includes minimum bias events, as well as decays of both beauty and charm. To
450 ensure that the timing is not biased as a function of load on the lxplus node used, provide
451 both the event loop and GaussGen algorithm timings, which allow for normalization to
452 non-changing algorithms. We report also the individual sequence timing for minimum
453 bias events in Table 2.

454 We see that on the whole, the timing of the event loop itself is $\mathcal{O}(10\%)$ of the full
455 simulation time. This factor is *only* on the Gauss + Boole itself, and does not include

Table 1: Timing in ms of the standard DELPHES sequence in comparison to GAUSS with and without simulation applied. All tests were performed on lxplus with the default options for each configuration. All have been run using PYTHIA 8. The values reported as the mean clock time from the TimingAuditor.

Decay File	DELPHES Sequence	GaussGen	Event Loop	GAUSS generation only; MainEventSeq	GaussGen	Event Loop	GAUSS with Simulation MainEventSeq	Gauss Gen	Event Loop
Minimum Bias (30000000)	5211.268	0.193	5578.220	103.685	0.148	163.958	33205.383	1.838	33743.742
$B^0 \rightarrow \pi^+ \pi^-$ (11102013)	4687.377	0.276	45952.051	4687.377	0.276	45952.051	37975.605	1.312	71846.844
$D^{*+} \rightarrow D^0 \pi^+$, $D^0 \rightarrow K^- \pi^+ \pi^- \pi^+$ (27265000)	4839.892	0.248	6551.347	1322.671	0.172	1408.644	58232.062	0.296	60298.934
$B^+ \rightarrow K^{*+} \mu^-$ (11114001)	4660.982	0.258	20253.385	16744.717	0.181	16829.184	56409.137	0.331	73254.391
$B_s^0 \rightarrow \phi \gamma$ (13102201)	4439.395	0.210	25153.633	20118.775	0.174	20195.631	52773.910	0.396	73449.562

Table 2: Individual contributions to the DELPHES sequence for min bias events generated with PYTHIA 8, as reported by the timing monitor. We also list the Gauss sequence and GaussGen for direct comparison with Table 1.

Step	Mean User Time (ms)	Mean Clock Time	min	max	sigma
InitDelphes	0.250	0.285	0.095	1.6	0.18
DelphesAlg	4111.200	4111.615	0.569	16470.6	3491.46
DelphesHist	3.800	3.784	0.026	11.6	2.81
DelphesProto	0.800	1.020	0.041	3.1	0.57
DelphesRecoSummary	0.000	0.021	0.010	0.3	0.02
DelphesParticleId	532.950	533.180	0.023	17297.0	1280.64
ChargedProtoParticleAddRich	0.150	0.093	0.008	1.9	0.13
ChargedProtoParticleAddMuon	0.050	0.038	0.007	0.9	0.06
ChargedProtoCombineDLLsAlg	0.000	0.050	0.005	0.5	0.04
DelphesCaloProto	546.500	546.458	0.040	3248.9	513.52
DelphesTuple	13.650	14.138	0.053	47.7	11.90
BooleInit	0.300	0.306	0.109	2.0	0.22
PGPrimaryVertex	0.100	0.025	0.017	0.3	0.02

456 the running of BRUNEL or any other possible steps. Even more striking, comparing
457 $D^0 \rightarrow K^- \pi^+ \pi^- \pi^+$ for full simulation, the speedup is a factor of 12 for the total event loop.
458 This can be attributed almost entirely to the lack of particles generated in interactions.

459 8 Conclusion

460 We have presented the incorporation and deployment of a DELPHES based simulation
461 in LHCb. Algorithms for the full simulation of events taking a fraction of the time of
462 traditional simulation have been implemented and have been shown to produce full physics
463 output on the timescale of the traditional simulation phase alone. Future improvements
464 include the final tunings of the primary vertex smearing for all years, which can then be
465 used as input at configuration time, and as well individual tunings for the calorimeter and
466 PID for each year of datataking. Future collaboration with and feedback from physics
467 working groups is paramount to have the final parameterizations for physics productions
468 provided.

469 The presented framework here is only valid for signal particles generated from a
470 decay file or any other particle produced by PYTHIA. This does not adequately model
471 background distributions. For this use, either a hybrid generation of signal only using
472 DELPHES combined statistically with a background sample or a different solution is
473 warranted. We note this to be completely clear in the application of this tool.

474 Acknowledgements

475 We thank Marco Cattaneo, Marco Clemencic, Gloria Corti and Domink Müller for their
476 technical help in all parts of this project. We thank Agnieszka Dziurda and Lucia Grillo
477 for the help with the development of the tracking parameterizations. We also thank
478 Concezio Bozzi for general support and guidance.

479 References

- 480 [1] DELPHES 3, J. de Favereau *et al.*, *DELPHES 3, A modular framework for fast*
481 *simulation of a generic collider experiment*, JHEP **02** (2014) 057, arXiv:1307.6346.
- 482 [2] M. Clemencic *et al.*, *The LHCb simulation application, Gauss: Design, evolution and*
483 *experience*, J. Phys. Conf. Ser. **331** (2011) 032023.
- 484 [3] Geant4 collaboration, J. Allison *et al.*, *Geant4 developments and applications*, IEEE
485 Trans. Nucl. Sci. **53** (2006) 270.
- 486 [4] LHCb collaboration, A. A. Alves Jr. *et al.*, *The LHCb detector at the LHC*, JINST **3**
487 (2008) S08005.
- 488 [5] L. Anderlini, D. Derkach, N. Kazeev, and A. Maevskiy, *Artificial Neural Networks*
489 *for the Ultra-Fast Simulation of the LHCb experiment and its upgrade*, Tech. Rep.
490 LHCb-INT-2019-014. CERN-LHCb-INT-2019-014, CERN, Geneva, May, 2019.